Supplementary Information to: Rheology of bi-disperse dense fiber suspensions

Monsurul Khan,[1] Ria D. Corder,[1,2] Kendra A Erk,[2] and Arezoo M. Ardekani[1]

[1] *School of Mechanical Engineering, Purdue University, West Lafayette, Indiana 47907, USA*
[2] *School of Materials Engineering, Purdue University, West Lafayette, Indiana 47907 USA*

(Dated: June 15, 2023)

In this document We provide further information about the measurement of the fiber dimensions and density Matching of Nylon Fibers to the Suspending Medium. Moreover, we include details about the numerical method, used in these simulations.

Measurement of Average Fiber Dimensions

Suspensions containing 10 v% of small (nominal length = 0.6 mm, nominal diameter = 49.8 μm) or large (nominal length = 1.0 mm, nominal diameter = 49.8 μm) were prepared in the density-matched suspending medium (54 v% glycerol, 46 v% deionized water) as described in the Experimental Section. Suspended fibers were imaged at 4X magnification using an Olympus BX41 microscope. The lengths, diameters, and aspect ratios of 50 fibers per type were obtained using ImageJ. The fiber distributions are shown in Figure S1.

Density Matching of Nylon Fibers to the Suspending Medium

Glycerol/water mixtures containing 52-56 v% glycerol were prepared in scintillation vials in 5 mL quantities via magnetic stirring at room temperature. Next, 0.05 g of large nylon fibers (nominal length = 1.0 mm, nominal diameter = 49.8 μm) were added to each vial and allowed to mix for 30 min, after which the suspensions were allowed to rest overnight at room temperature to observe whether the nylon fibers remained suspended. An image of the nylon fiber suspensions obtained the next day (Figure S2) reveals that a 54 v% glycerol, 46 v% water mixture is density-matched to the nylon fibers. At lower glycerol contents (52-53 v% glycerol), the fibers are denser than the suspending medium and sink to the bottom of the vial. At higher glycerol contents (55-56 v% glycerol), the fibers are less dense than the suspending medium and float at the top of the vial.

Numerical method

The fluid-solid coupling is achieved using the Immersed Boundary Method (IBM) [1]. In the IBM, the geometry of the object is represented by a volume force distribution $\mathbf{f}$ that mimics the effect of the object on the fluid. In this method, two sets of grid points are needed: a fixed Eulerian grid $\mathbf{x}$ for the fluid and a moving Lagrangian grid $\mathbf{X}$ for the flowing deformable structure as shown in figure S3. Each fiber has its own Lagrangian coordinate system.

In this study we assume the fibers to be neutrally buoyant, so equation of motion of fiber is

$$\frac{\partial^2 \mathbf{X}}{\partial t^2} = \frac{\partial^2 \mathbf{X}_{fluid}}{\partial t^2} + \frac{\partial}{\partial s}(T\frac{\partial \mathbf{X}}{\partial s}) - B\frac{\partial^4 \mathbf{X}}{\partial s^4} - \mathbf{F} + \mathbf{F}^f, \tag{1}$$

where the LHS term is the acceleration of the fiber, and the RHS consists of the acceleration of the fluid particle at the fiber location and the different forces acting on the fibers. Here, s is the curvi-linear coordinate along the fiber, $\mathbf{X} = (x(s,t), y(s,t), z(s,t))$ is the position of the Lagrangian points on the fiber axis, T is the tension, B is the bending rigidity, $\mathbf{F}$ is the fluid-solid interaction force, $\mathbf{F}^f$ is the net inter-fiber interaction.

To solve for the fiber position in equation 1, we first solve the Poisson's equation for tension as:

$$\frac{\partial \mathbf{X}}{\partial s}.\frac{\partial^2}{\partial s^2}(T\frac{\partial \mathbf{X}}{\partial s}) = \frac{1}{2}\frac{\partial^2}{\partial t^2}(\frac{\partial \mathbf{X}}{\partial s}.\frac{\partial \mathbf{X}}{\partial s}) - \frac{\partial^2 \mathbf{X}}{\partial t \partial s}.\frac{\partial^2 \mathbf{X}}{\partial t \partial s} - \frac{\partial \mathbf{X}}{\partial s}.\frac{\partial}{\partial s}(\mathbf{F}^a + \mathbf{F}^b + \mathbf{F}^f - \mathbf{F}), \tag{2}$$

where $\mathbf{F}^a = \frac{\partial^2 \mathbf{X}_{\mathbf{fluid}}}{\partial t^2}$ is the acceleration of the fluid particle at the fiber location and $\mathbf{F}^b = -B\frac{\partial^4 \mathbf{X}}{\partial s^4}$ is the bending force. The effect of the moment exerted by the fluid on the freely suspended fibers also appears in equation 2 and has been discussed elsewhere [2].

As the fibers are freely suspended in the fluid medium, we impose zero force, torque and tension at the free ends.

$$\frac{\partial^2 \mathbf{X}}{\partial s^2} = 0, \frac{\partial^3 \mathbf{X}}{\partial s^3} = 0, \text{ and } T = 0. \tag{3}$$

At each time step, the fluid velocity is first interpolated onto the Lagrangian grid points using the smooth Dirac delta function, δ [3]:

$$\mathbf{U}_{ib} = \int_V \mathbf{u}(\mathbf{x}, t)\delta(\mathbf{X} - \mathbf{x})dV, \tag{4}$$

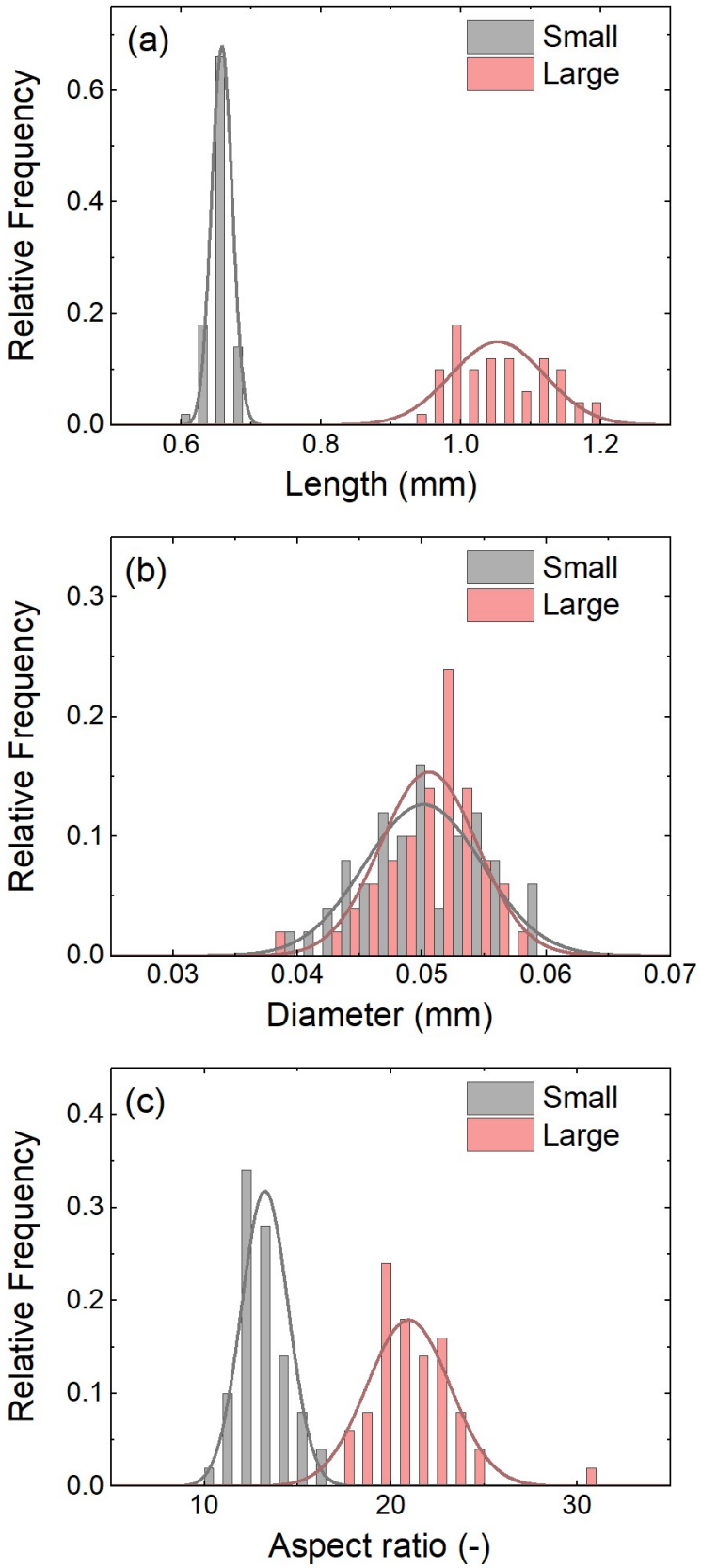

FIG. S1: Fiber length (a), diameter (b), and aspect ratio (c) distributions for the small and large nylon fibers used in this work.

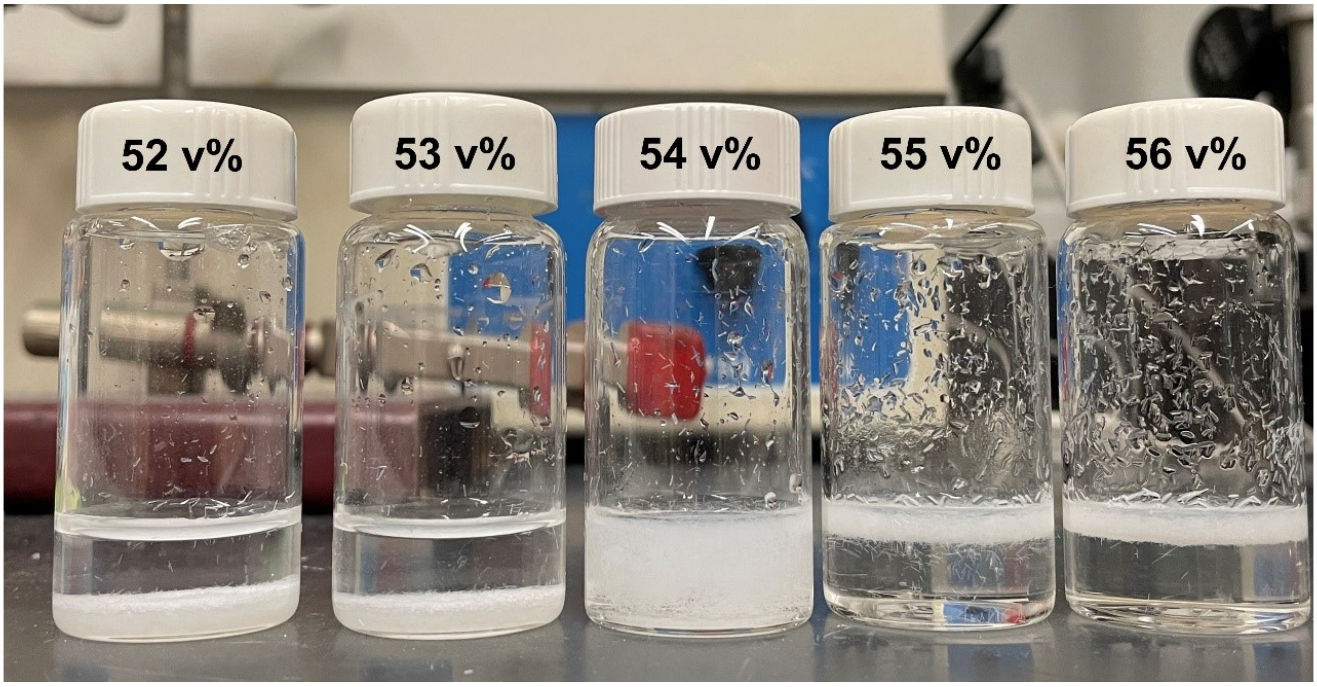

FIG. S2: Pictures of large nylon fibers suspended in glycerol/water mixtures containing varying v% glycerol and allowed to rest overnight.

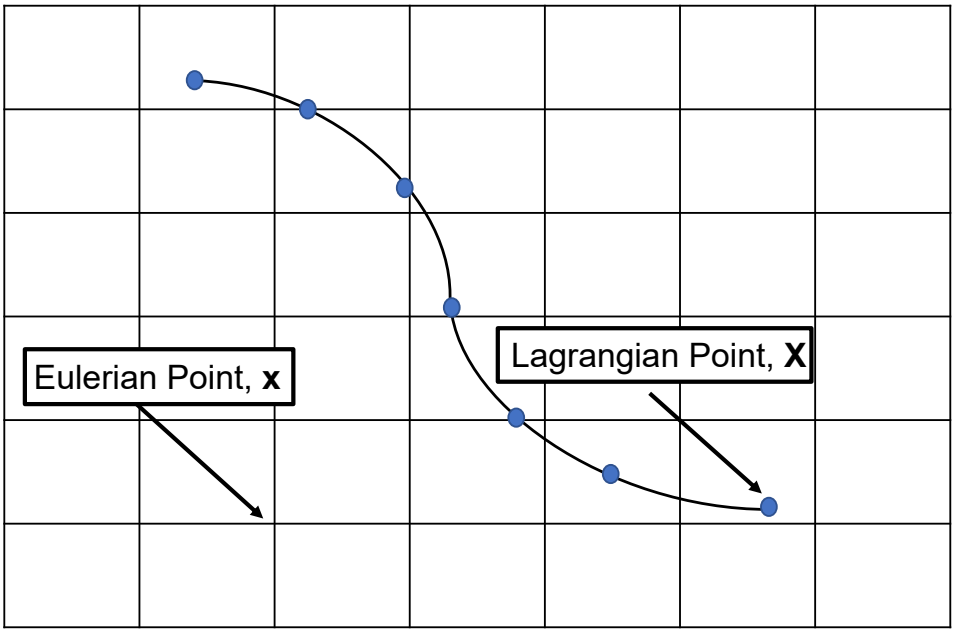

FIG. S3: Schematic of the Eulerian and the Lagrangian grids. The blue dots denote the Lagrangian points through which the position of the fibers are defined.

The fluid and solid equations are then coupled by the fluid-solid interaction force,

$$\mathbf{F} = \frac{\mathbf{U} - \mathbf{U}_{ib}}{\Delta t}, \tag{5}$$

where $\mathbf{U}_{ib}$ is the interpolated fluid velocity on the Lagrangian points defining the fibers, $\mathbf{U}$ is the velocity of the

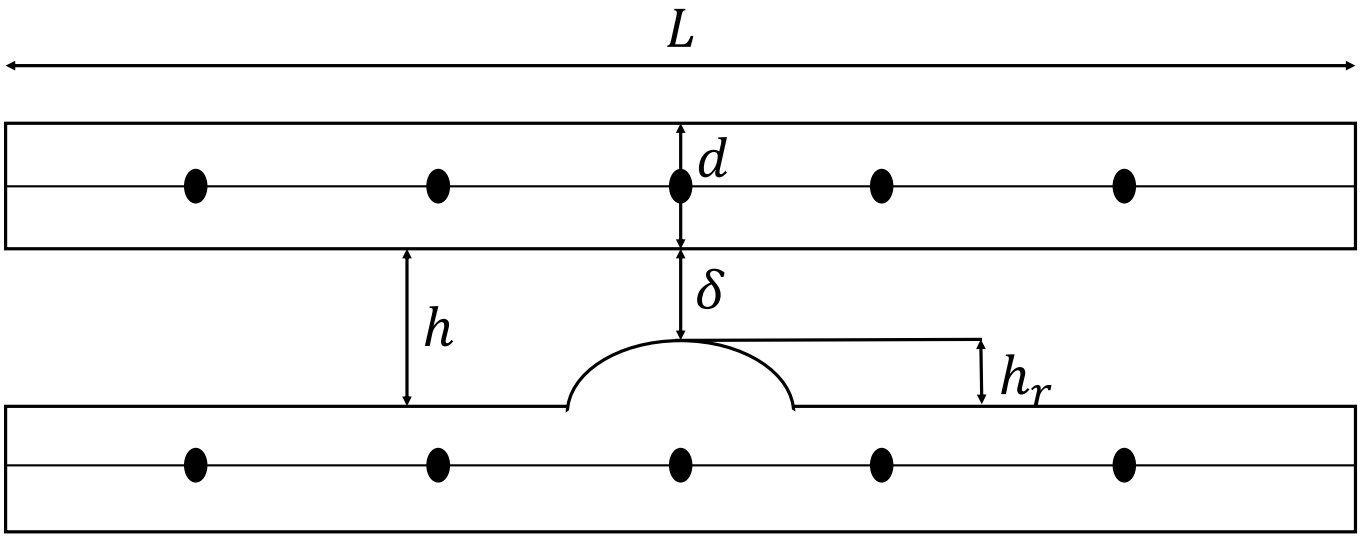

FIG. S4: A sketch of the roughness model, L and d are the length and diameter of the fiber, respectively, h_r is the roughness height, and $\delta = h - h_r$ is the surface overlap. Contact occurs when $\delta \leq 0$. Dots along the axes of the fibers indicate Lagrangian points.

Lagrangian points and Δt is the time step. The Lagrangian force is then extrapolated onto the fluid grid by

$$\mathbf{f}(\mathbf{x}, t) = \frac{\pi}{4} r_p^2 \int_L \mathbf{F}(\mathbf{X}, t)\delta(\mathbf{X} - \mathbf{x})ds. \tag{6}$$

Here $r_p = d/l$, is the slenderness ratio of the fiber, which is the inverse of its aspect ration defined as $A = l/d$.

Lubrication interactions

To accurately resolve the lubrication interactions between the fibers when the inter-fiber gap falls below a few grid-sizes, we use the lubrication correction model of [4]. The lubrication force model is based on two infinite cylinders for two different cases: the cylinders can be parallel or at an arbitrary angle. The first-order approximation of the lubrication force for the non-parallel case was derived by [5] and is given as follow:

$$\mathbf{F}_1^l = \frac{-12}{\mathrm{Re}\sin\alpha}\frac{\dot{\mathbf{h}}}{h}, \tag{7}$$

here h is the shortest distance between the cylinders, $\dot{\mathbf{h}}$ is the relative normal velocity between the closest points on the fibers, and α is the contact angle. The first order approximation of the lubrication force per unit length between parallel cylinders was derived by [6]:

$$\begin{aligned} &\mathbf{F}_2^l = \tfrac{-4}{\pi \mathrm{Re} r_p^2}\left(A_1 + A_2\tfrac{h}{a}\right)\left(\tfrac{h}{a}\right)^{-3/2}\dot{\mathbf{h}}, \\ &A_1 = 3\pi\sqrt{2}/8, A_2 = 207\pi\sqrt{2}/160, \end{aligned} \tag{8}$$

here a is the cylinder radius ($a = d/2$). Based on equations 7 and 8, the following approximation of the lubrication force for two finite cylinders is [4]:

$$\mathbf{F}^l = \min\left(\mathbf{F}_1^l/\Delta s, \mathbf{F}_2^l\right). \tag{9}$$

The force for the non-parallel case is divided by the Lagrangian grid spacing Δs to calculate the force per unit length. The numerical method implemented to calculate the lubrication force is discussed in [2], and hence is not repeated here. As the distance between the fibers becomes the order of the mesh size, hydrodynamic interactions are not well resolved; to address this issue, we introduce a lubrication correction force [4]. When the shortest distance between two Lagrangian points becomes lower than $d/4$, we introduce lubrication correction force as: $\mathbf{F}^{lc} = \mathbf{F}^l - \mathbf{F}_0^l$, where F_0^l is the lubrication force at a $d/4$ distance.

The lubrication forces diverge as the minimum inter-fiber separation decreases, and theoretically should prevent the fibers from coming into direct contacts. However, the thin lubrication film between close fibers can break because of the presence of irregularities on their surfaces leading to a direct contact between the fibers and hence, contact forces.

Stress and bulk rheology calculations

The bulk stress in the suspension is required to quantify the rheological properties of the suspension. The total stress in the suspension in terms of contributions from hydrodynamics and fiber stresses in the dimensionless form is [7]:

$$\Sigma_{ij} = Re\left[\frac{1}{V}\int\limits_{V-\sum V_f}\left(-p\delta_{ij}+\frac{2}{Re}e_{ij}\right)dV+\frac{1}{V}\sum_{1}^{n}\int\limits_{V_f}\sigma_{ij}dV-\frac{1}{V}\int\limits_{V}u'_i u'_j dV\right]. \tag{10}$$

Here, V is the total volume, V_f is the volume occupied by each fiber, $e_{ij}=\frac{\partial u_i}{\partial x_j}+\frac{\partial u_j}{\partial x_i}$ represents the strain rate tensor, and $\boldsymbol{u}'$ is the velocity fluctuation. σ_{ij} is the fiber stress [8]. The dimensionless total stress consists of the fluid bulk stress and the stress generated by the presence of fibers and the interactions between them. So, the total stress (Σ_{ij}) can be written as

$$\Sigma_{ij} = \Sigma^0_{ij} + \Sigma^f_{ij}, \tag{11}$$

$$\begin{aligned}\Sigma^0_{ij} &= \tfrac{Re}{V}\int\limits_{V-\sum V_f}\left(-p\delta_{ij}+\tfrac{2}{Re}e_{ij}\right)dV,\\ \Sigma^f_{ij} &= \tfrac{Re}{V}\sum\int\limits_{V_f}\sigma_{ij}dV-\tfrac{Re}{V}\int\limits_{V}u'_i u'_j dV.\end{aligned} \tag{12}$$

Here, Σ^0_{ij} is the viscous fluid stress and results in a dimensionless contribution of 1 (or $\eta\dot{\gamma}$ in the dimensional form) in a simple shear flow after subtracting the isotropic fluid pressure. Σ^f_{ij} is the stress generated by the presence of fibers and inter-fiber interactions. The fiber stress σ_{ij} can be decomposed into two parts:

$$\int\limits_{V_f}\sigma_{ij}dV = \int\limits_{A_f}\sigma_{ik}x_j n_k dA - \int\limits_{V_f}\frac{\partial\sigma_{ik}}{\partial x_k}x_j dV, \tag{13}$$

where A_f represents the surface area of each fiber and $\mathbf{n}$ is the unit surface normal vector on the fiber pointing outwards. The first term is called the stresslet, and the second term indicates the acceleration stress [9]. The second term is identically zero for neutrally buoyant fibers when the relative acceleration of the fiber and fluid is zero. $\sigma_{ik}n_k$ is simply the force per unit area acting on the fibers [8]. Hence, for slender bodies, $\sigma_{ik}n_k$ can be rewritten as:

$$\int\limits_{A_f}\sigma_{ik}x_j n_k dA = -r_p^2\int\limits_{L}F_i x_j ds, \tag{14}$$

F_i is the fluid solid interaction force as defined in equation 5. The term r_p^2 arises from choosing the linear density instead of the volume density in the characteristic force scale. Finally, the total fiber stress is defined as:

$$\Sigma^f_{ij} = -\frac{Rer_p^2}{V}\sum_{1}^{n}\int\limits_{L}F_i x_j ds - \frac{Re}{V}\int\limits_{V}u'_i u'_j dV. \tag{15}$$

From the results of our simulations, we observe that, the last term related to the velocity fluctuations are very small compared to the stresslet and can be neglected for the range of Reynolds number considered here. The calculated bulk stress tensor can now be used to quantify rheological properties of the suspensions.

There are three main contributions to the bulk stress: 1) the hydrodynamic contribution Σ^h_{ij}, 2) the contact contribution Σ^c_{ij}, and 3) the non-contact contribution Σ^{nc}_{ij}. The contact and non-contact contributions can be calculated from the ensemble average of the contact and non-contact stresslets respectively given by:

$$\begin{aligned}\Sigma^c_{ij} &= -\tfrac{Rer_p^2}{V}\sum_{1}^{n}\textstyle\int_L F_i^c x_j ds,\\ \Sigma^{nc}_{ij} &= -\tfrac{Rer_p^2}{V}\sum_{1}^{n}\textstyle\int_L F_i^{nc} x_j ds.\end{aligned} \tag{16}$$

Thus, the hydrodynamic contribution can be simply obtained as $\Sigma^h_{ij} = \Sigma_{ij} - \Sigma^c_{ij} - \Sigma^{nc}_{ij}$. This splitting of the total stress allows us to track the variations in the contributions from different mechanisms to the observed rheological behavior of the suspension with varying parameters, e.g., $\eta^h_r = \Sigma^h_{xy}$, $\eta^c_r = \Sigma^c_{xy}$, and $\eta^{nc}_r = \Sigma^{nc}_{xy}$ are the hydrodynamic, the contact and non-contact contributions to the relative viscosity η_r, respectively.

[1] C. S. Peskin, Flow patterns around heart valves: a numerical method, Journal of computational physics **10**, 252 (1972).

[2] A. A. Banaei, M. E. Rosti, and L. Brandt, Numerical study of filament suspensions at finite inertia, Journal of Fluid Mechanics **882** (2020).

[3] A. M. Roma, C. S. Peskin, and M. J. Berger, An adaptive version of the immersed boundary method, Journal of computational physics **153**, 509 (1999).

[4] S. B. Lindström and T. Uesaka, Simulation of semidilute suspensions of non-brownian fibers in shear flow, The Journal of chemical physics **128**, 024901 (2008).

[5] Y. Yamane, Y. Kaneda, and M. Dio, Numerical simulation of semi-dilute suspensions of rodlike particles in shear flow, Journal of non-newtonian fluid mechanics **54**, 405 (1994).

[6] J. Kromkamp, D. T. Van Den Ende, D. Kandhai, R. G. Van Der Sman, and R. M. Boom, Shear-induced self-diffusion and microstructure in non-brownian suspensions at non-zero reynolds numbers, Journal of fluid mechanics **529**, 253 (2005).

[7] J. Wu and C. K. Aidun, A method for direct simulation of flexible fiber suspensions using lattice boltzmann equation with external boundary force, International Journal of Multiphase Flow **36**, 202 (2010).

[8] G. Batchelor, The stress generated in a non-dilute suspension of elongated particles by pure straining motion, Journal of Fluid Mechanics **46**, 813 (1971).

[9] E. Guazzelli and J. F. Morris, *A physical introduction to suspension dynamics*, Vol. 45 (Cambridge University Press, 2011).